Materials Separation by Dielectrophoresis

by

Ambuj Daya Sagar

B. Tech. Mechanical Engineering,
Indian Institute of Technology, Delhi (1985)

M.S. Aerospace Engineering,
University of Michigan, Ann Arbor (1986)

Submitted to the Department of Materials Science
and Engineering in partial fulfillment of the requirements
for the Degree of Master of Science

at the

Massachusetts Institute of Technology

June 1989

Signature of Author.....
Department of Materials Science and Engineering
May 12, 1989

Certified by.....
Robert M. Rose
Professor, Materials Science and Engineering

Accepted by.....
Samuel M. Allen
Chairman, Department Committee on Graduate Students

Materials Separation by Dielectrophoresis

by

Ambuj D. Sagar

Submitted to the Department of Materials Science and Engineering
on May 12, 1989 in partial fulfillment of the requirements
for the Degree of Master of Science.

Abstract

The feasibility of vacuum dielectrophoresis as a method for particulate materials separation in a microgravity environment was investigated. Particle separations were performed based on differences in densities as well as both in densities and dielectric constants, in a specially constructed miniature drop tower with a residence time of ca. 0.3 seconds. Particle motion in such a system is independent of size and based only on density and dielectric constant for a given electric field. The observed deflections exceeded those predicted by the theory based on a single particle analysis. A modified analysis which takes into account field perturbation effects by the dielectric particles was developed to investigate these results. This analysis indicates that the enhanced separations are probably due to multiparticle effects which are not negligible in a large space density of particles.

Thesis supervisor: Robert M. Rose

Title: Professor of Materials Science
and Engineering

Table of Contents

List of Tables

List of Figures

Acknowledgements

It was a real privilege and pleasure to work with Prof. Rose. His deep insight into the subject matter and philosophy of tackling research problems was a source of constant inspiration. Add to this his informal and supportive attitude and inimitable sense of humor and the result was, for me, an extremely enjoyable and educative experience.

Thanks also to Leslie, for helping me to acclimatize to MIT as a new graduate student, for helping me in an uncountable number of ways on a day to day basis, for all the great conversations...

I would also like to thank I. M. Puffer for building the experimental setup and for aiding me subsequently in the lab, and Len Sudenfield for his help with the SEM photography. Thanks also to Guenter Arndt, Bruce Russell and the other folks in the Welding Lab.

This work was supported by NASA via Grant number NSG-7645 to the MIT Materials Processing Center.

Last but not the least, I want to express my thanks and gratitude to my family for their love, support and encouragement without which I would not be here.

Chapter 1 : Introduction

The two major electrokinetic techniques which have been applied to materials separation are electrophoresis and dielectrophoresis. The former technique, along with its variations such as isotachophoresis and isoelectric focussing, involves the migration of charged matter under the influence of a uniform, steady electric field. Therefore, it is used to separate materials which already carry a charge or can be made to do so in a controlled manner, and for this reason finds applications primarily in the separation of biological materials based on charge and/or size. Dielectrophoresis, on the other hand, is the translational motion of neutral matter caused by polarization effects in a nonuniform (steady or oscillating) electric field. The electrical force on any object undergoing dielectrophoresis is directly related to its volume and polarizability, which is some function of its complex electrical permittivity, for a given medium and electric field.

Dielectrophoresis has been applied to separating a variety of materials. Pohl and Schwar[1,2] demonstrated the separations of organic and inorganic powders in and from liquid dielectrics. The yield was found, in agreement with theory, to depend on a variety of factors such as field strength and gradient, particle size, etc. With further modifications to this apparatus, it was also possible to utilize this technique to allow continuous separations[3]. In this case, however, it was noted that the obtained efficiency of the separations actually exceeded the theoretically expected values. Another interesting study by Crane et al.[4] allowed the separations of live yeast cells from dead ones based on their different electrical responses. In fact, due to the extreme sensitivity of biological materials to

electrical fields, dielectrophoresis may yet find use as a method for separating or purifying them on the basis of their type and state. As an aside, it is worth mentioning that apart from these numerous applications involving materials separations, this technique has been utilized to obtain information about physical and transport properties of macromolecules on the basis of their mobility in nonuniform fields[5,6].

It should be noted that past work utilizing dielectrophoresis has been carried out in some kind of a fluid medium which serves the dual purpose of increasing the residence times of the material in the separation cell, as well as enhancing the forces acting upon them. However, the strength of the electric field is limited due to the susceptibilty of the medium to breakdown. Also, the presence of such a medium leads to fluid phenomena, driven by gravity, thermal effects or otherwise, such as convection, which are extremely difficult to eliminate under normal circumstances, and to which dielectrophoresis is extremely vulnerable due to the weak nature of its operating force.

Parts of this problem, however, could be eliminated or at least reduced in a microgravity environment. Even if a supporting medium were to be used, the elimination of the gravity-driven phenomena would lead to a substantial improvement in the viability of such a technique. It has been shown with other electrokinetic materials processing techniques, such as those mentioned earlier, that the absence of certain convective disturbances and boundary instabilities in a microgravity environment offers significant quantitative and qualitative advantages over similar processes carried out in normal gravity. For example, during free fluid particle electrophoresis

carried out on the Apollo 16, it was possible to achieve extremely sharp boundaries during the migration of polystyrene latex particles[7]. Also, in electrokinetic experiments carried out on the Apollo-Soyuz test project, very high resolution was obtainable during the separation of cells of different types[8].

Still, it is not possible to totally eliminate certain fluid phenomena. On the other hand, a process carried out in the absence of a fluid medium would not suffer from these problems, but in such a case, the residence times of any material under the influence of normal gravity in a cell of reasonable size is too small to allow any commercially significant separations. A microgravity/low gravity environment would allow large residence times in the separation cells, leading to very efficient separations.

Thus, vacuum dielectrophoresis presents itself as an excellent candidate for particulate separations on either the space station or the surface of the moon. This technique, in which the separations can be based on differences in density or dielectric constant or a combination of both, is, in a way, analogous to classical mineral separation technologies, where the separations are based on density differences. Furthermore, it obviates the need for water and other reagents which are necessary for conventional separations. The basic apparatus is also quite simple, since not much more than two electrodes and a power supply are required.

The goal of the present investigation was to evaluate the feasibility of dielectrophoresis as a viable space processing technique. An electric field was applied to a mixture of powders falling in a vacuum under the influence of gravity. Experimental measurements of the extent of

separations, if any, were used to provide information for our investigative purposes.

Chapter 2 : Theoretical Background

Particles used in the experiments had either microspherical or slightly irregular geometries, but an assumption was made that all particles could be considered spherical, in order to develop a quantitative analysis. The following theory underlying dielectrophoresis is mainly drawn from refs. 9 and 10.

Under the influence of an electric field, **E**, any dielectric body develops an induced moment. If we call this dipole moment vector to be μ, then the body experiences a force **F**,

$$\mathbf{F} = (\mu.\nabla)\,\mathbf{E}$$

Furthermore,

$$\mu = (\alpha\, v)\,\mathbf{E}$$

for an isotropically, homogeneously, and linearly polarizable body of volume v and (tensor) polarizability α.

For the case of a small sphere of radius c of dielectric permittivity ε_2 placed in a dielectric medium of dielectric permittivity ε_1 the external field distribution is distorted to give a field interior to the sphere

$$\mathbf{E}_i = \frac{3\,\varepsilon_1}{\varepsilon_2 + 2\,\varepsilon_1}\,\mathbf{E}$$

The polarization, **P**, (i.e. the dipole moment per unit volume) in the sphere is, by definition:

$$\mathbf{P} = \alpha\,\mathbf{E} = (\varepsilon_2 - \varepsilon_1)\,\mathbf{E}_i$$

$$= 3\varepsilon_1 \frac{(\varepsilon_2 - \varepsilon_1)}{(\varepsilon_2 + 2\varepsilon_1)} \mathbf{E}$$

Thus, the total induced moment is given by

$$\mu = 4\Pi c^3 \varepsilon_1 \frac{(\varepsilon_2 - \varepsilon_1)}{(\varepsilon_2 + 2\varepsilon_1)} \mathbf{E}$$

The translational force **F**, on the sphere is

$$\mathbf{F} = 2\Pi c^3 \varepsilon_1 \frac{(\varepsilon_2 - \varepsilon_1)}{(\varepsilon_2 + 2\varepsilon_1)} \nabla |\mathbf{E}|^2$$

which drives it, for $\varepsilon_2 > \varepsilon_1$ into the region of the highest field strength, and for $\varepsilon_2 < \varepsilon_1$ into the region of the lowest field strength.

Since $\varepsilon_1 = \varepsilon_0 K_1$ and $\varepsilon_2 = \varepsilon_0 K_2$, we have:

$$\mathbf{F} = 2\Pi c^3 \varepsilon_0 K_1 \frac{K_2 - K_1}{K_2 + 2K_1} \nabla |\mathbf{E}|^2$$

For a concentric cylindrical electrode configuration (Fig. 2), with the inner electrode of radius r_1 at potential V_1 and the outer electrode of radius r_2 at ground potential, we have at some intermediate radius r (Appendix II):

$$\nabla |\mathbf{E}|^2 = \frac{-2V_1^2}{r^3 [\ln(r_1/r_2)]^2} \mathbf{r}_0$$

Therefore the net electric force on a sphere placed at this radial position is

$$\mathbf{F} = 4\Pi c^3 \varepsilon_0 K_1 \frac{K_2 - K_1}{K_2 + 2K_1} \frac{V_1^2}{r^3 [\ln(r_1/r_2)]^2} \mathbf{r}_0$$

If the body is placed in vacuum, as in our case, there is no other force acting on it in the non-vertical direction. Thus the horizontal motion of the body is governed only by the operating dielectrophoretic force.

If the sphere is of density ρ, and mass M,

$$M = \frac{4}{3}\Pi c^3 \rho$$

From this one obtains the acceleration experienced by the particle

$$\mathbf{a} = -3\frac{\varepsilon_0}{r} K_1 \frac{K_2 - K_1}{K_2 + 2K_1} \frac{V_1^2}{r^3 [\ln(r_1/r_2)]^2} \mathbf{r}_0$$

This expression is specifically applicable only for the system considered above since the electric field is a function of the electrode configuration. For a given geometry, this acceleration is dependent on the density of the particle, its relative dielectric constant and that of the medium, and the gradient of the square of the electric field.

For $K_2 > K_1$, the magnitude of the acceleration increases with K_2 for a fixed K_1 and r. Also, it should be noted that under this condition, the limiting values of $K_1 [(K_2 - K_1)/(K_2 + 2K_1)]$ are 0 (for $K_2 = K_1$) and 1 (for $K_2 \to \infty$). Thus beyond a certain extent, increasing K_2 does not really appreciably increase the force acting on the body. The acceleration experienced by the particle, however, decreases as the density increases for fixed K_2 and K_1 independent of the size of the body. In effect, the magnitude of the acceleration is controlled by two bulk properties of the material undergoing dielectrophoresis, the density and the dielectric constant for fixed experimental conditions.

The direction of motion of the body under consideration is determined by the relative magnitudes of K_2 and K_1. Since for such a system of coaxial cylindrical electrodes, the direction of the gradient of the square of the magnitude of the electric field is radially inwards, for $K_2 > K_1$, the acceleration experienced will be towards the inner electrode and vice versa. Thus, through proper choice of the relevant materials and the medium, it should be possible to maximize the relative motion between the different materials, allowing for suitable separations.

Chapter 3 : Experimental Methods

For the purpose of our investigations, a vacuum dielectrophoretic separation apparatus was designed and constructed. The separator (Fig. 1) was based on a six-foot drop column which was a thick-walled glass tube with an internal diameter of four inches. The electrode configuration used was concentric cylindrical (Fig. 2), the outer electrode (grounded) being a thin layer of gold deposited on the inside wall of the column, and the inner electrode (connected to the energizing system) being a stainless steel tube 0.5 inches in diameter. The base of the tube was fixed on to a small chamber with a plenum for pumping and vacuum instrumentation. This plenum chamber was in turn mounted on a platform with rubber dampers on the bases of the legs which allowed for isolating the whole system from external vibrations, if any. There were also levelling screws on the legs which allowed adjustments to make the drop tower exactly vertical.

The drop device for releasing the powders (which were to be separated based on their bulk properties) was placed on top of this separation column. These powders were held in a cavity by a spring-loaded conical brass piece. The mixture was released in a gradual vibration-free manner through an annular cavity which was accessible only as the conical piece was depressed under the action of a push rod driven by a cam which was rotated by a motor through a worm-gear attachment.

Since the annular opening was much larger than the size of the particles, the mixtures tended to spread during the fall and tended to assume a uniform distribution all across the cross-section of the separator rather than a narrow, annular distribution, as one expected (and hoped for).

For this reason a simple collimator, for controlling the lateral spread of the powders was designed and placed between the drop device and the separation column.

This consisted of a brass tube, thirty inches long with an internal diameter of four inches (Fig. 3). Inside this tube were four equally spaced plates with a slit 60 mils wide milled in each plate, tangential to a circle of radius 0.75 inches. The plates were held in place, with all the slits carefully aligned, by a brass rod. This collimator constrained the spread of the powders so that the falling powders, under the absence of any radial forces landed in a slit pattern about three to five mm. wide at the base of the drop tower.

To collect the powders at the end of the fall, a substrate coated with an adhesive was placed in the plenum chamber through an access plate at the bottom of the drop column. This substrate consisted of a brass plate 2.5 inches long and one inch wide which in turn was clamped to an auxiliary plate fixed to the front access plate. Adhesives were chosen to be free of any solvents (which would obviously volatilize at the low pressures involved) and also maintain their tackiness for a substantial period (as it took a few hours for the vacuum to develop and stabilize). For most of the qualitative work, high vacuum grease (Dow Corning) was used as the adhesive because of its extreme stability under low pressure and extraordinary tackiness. Subsequently, though, when the powder distribution was to be photographed for quantitative analysis purposes using a scanning electron microscope, Scotch Tape (3M) was preferred to the grease, even though it was less tacky. This was to avoid the decomposition of

the "adhesive' by the electron beam in the SEM, an obviously undesirable event.

The system was pumped by a Varian HSA air cooled 2 inch diffusion pump backed by a Duo Seal 5 cfm mechanical vacuum pump. Vacuum instrumentation consisted of a Varian 571 series Bayard-Alpert type standard range ionization gauge tube and a Varian 531 thermocouple gauge tube, both controlled by a Varian 843 Ratiomatic ionization gauge control. Ultimate vacuum achievable was between 1.0 E-06 to 1.0E-07 Torr.

A General Radio Type 1309-A variable output oscillator provided the basic electrical signal in the range 20 Hz-20 kHz. This was amplified by a Bogen MT-250C booster audio amplifier which delivered a maximum constant voltage output of 100 V rms at 250 Watts rms continuous. The final components of the energizing system were the high current transformers (Newton Engg. Services) with a step-up ratio of 100. Since power transformers for this range of frequencies and voltages are a problem, there were three transformers which between them spanned the whole audio range : NES 7286 for 20 Hz to 400 Hz, NES 7287 for 400 Hz to 6.5 kHz, and NES 7288 for 6.5 kHz to 20 kHz. Shielded cable was utilized for carrying the final electrical signal to the drop column to avoid any interferences from external sources. Thus the EMF capability of the system was 0-10 kV max rms at frequencies from 20 Hz to 20 kHz. This was measured using a high voltage probe and an oscilloscope. The calculated lateral accelerations for this electrode geometry and voltage were in the 0.001-0.005 g range.

A variety of powders (metals, ceramics, and polymers) were used in the experimental runs. Powders were selected on the basis of their

dielectric constants and density, the two properties which determined the effectiveness of the separation process as mentioned earlier. Care also had to be taken in the choice of particle size: particles which were too large led to a small numerical distribution on the substrate from which it was difficult to draw statistically significant conclusions. Particles which were too small tended to agglomerate which resulted in problems in the powders being released through the drop device. Also the weak operating (dielectrophoretic) force was not effective in separating clusters containing particles of both the mixture constituents. In general, chemical dispersing agents (anti-agglomerants) were not effective in vacuum.

In light of the above considerations, the powders chosen were in the range of 50-200 mesh sieve (i.e. 75-300 microns) preferably with a microspherical geometry, if available. These conformed with our theoretical assumptions and also dropped smoothly without agglomerating. The powders used for the test runs are listed with their relevant bulk properties in Table 1[3,11].

Before an experimental run, special care was taken to ensure the drop tower was perfectly vertical and the collimator slits were well aligned. During the experimental runs, the pressure in the system was lower than 1.0E-06 Torr. The voltage applied to the central electrode through the energizing system mentioned earlier was 10 kV rms at an operating frequency of 1 kHz. Care was taken to allow the oscillator to stabilize to provide a constant output. The choice of the operating frequency was arbitrary since all the test powders (except poly methyl methacrylate) had dielectric constants that were not a function of the frequency in the audio

range. The pumping system was switched off just previous to the actual drop to minimize the vibrations. The residence time of the powders during free fall through the separation column was circa 0.3 seconds. Preferably one of the constituents moved minimally in the field while the other exhibited a large radial movement. The former was then considered a reference, and the relative deflection of the second constituent measured. This experimental protocol of measuring the relative, and not the absolute movements, was chosen to avoid the uncertainty of positioning the substrate with respect to the collimator slits. As mentioned earlier, the lateral accelerations experienced by the particles is quite small, as a result of the weak nature of the operating force. This coupled with the small residence time of the powders in the drop tower allowed for very small deflections and as a result even a slight uncertainty in the position of the base plate to an external reference could have created havoc with the measurements.

Since the collimator filtered out a large fraction of the powders, two or three successive runs were made with the same mixtures without disturbing the system, so as to obtain a reasonably dense deposition on the substrate. In order to gain information about the particle distributions, the substrate, subsequent to the run, was coated with a 200 Å layer of gold, and high resolution photographs were taken on a scanning electron microscope (Cambridge).

Chapter 4 : Results and Discussion

Separations from a mixture of two particulate materials, based on differences in densities as well as both in densities and dielectric constants were achieved.

To analyze the experimental data, a grid was placed over the photographs obtained on the SEM (eg. Fig. 4), and the concentration of the particles across the width of the powder patterns were then obtained by visual count. These concentrations, C, normalized by the centerline value (i.e. the centerline corresponding to that specific material distribution) C_0 are plotted in Figs. 5-7. X represents the radial position from some arbitrary origin. It was not necessary to locate the actual origin of the powder distribution (the collimator slit) since as mentioned earlier only the relative, and not the absolute, movements of the powders were evaluated.

The centerline of the distributions of the particles which moved to a smaller extent in the field was set as a reference to measure the relative radial deflection of the other particles. The theoretical predictions of such deflections for the pair of materials constituting the given mixtures are also shown (also see Table 2).

Since the acceleration experienced by the particles is a very strong function of the radius, even small changes in the radial position could have a significant effect on the resulting motions. For this reason, measurements were made at the lengthwise center of the slit, i.e. the only portion of the slit at an actual radial distance of 0.75 inches from the center, which was the radius used in our theoretical calculations.

The edges of the powder distributions on the substrate had a shape characteristic of an error function. This is expected since the powder drop is a percolative process and the usual equations for diffusion should be applicable. In this case, the initial concentration profile of the powders is a square wave at the collimator slit. As the powders diffuse outwards during the free fall, the profile broadens out.

The separations obtained experimentally well exceeded those predicted by theory developed earlier in Chapter 2 for the motion of a particle under the influence of dielectrophoretic forces, as can be seen in Figures 5-7. Similar observations of the dielectrophoretic effect exceeding the theoretical predictions are reported by Pohl et al.[3] and attributed to a variety of multiparticle effects such as mutual dielectrophoresis which by allowing "pearl-chain" formation may lead to reduced drag of the particles through the medium[9] or by a "bunching" effect in which the presence of particle-particle and particle-field interactions may accentuate the dielectrophoretic force acting on the aggregates[3]. However, no definitive explanation for such observations has been reported in the literature. In our case, obviously, the high vacuum in the separation column eliminates the possibility of a reduction in the drag as a cause of the enhanced separations. Furthermore, it seems from the theory developed (Appendix II) in an attempt to evaluate the magnitude of the field perturbations resulting from these dielectric particles, that close proximity of the particles to each other may be the underlying reason for such observations.

Any dielectric particle has a dipole moment in the presence of an external electric field. The local electric field resulting from

this dipole can increase the magnitude of the total field to a significant extent within a distance of a few particle radii from its center. As a result, any particle within this region experiences the external and the secondary field which has the effect of magnifying the dielectrophoretic force acting on the particle. Thus, with a large space density of particles, the net operating force can be substantially larger than the theoretical predictions for a single particle in the field. In our experimental set-up, such an environment was created by the collimator which directed the particles to fall in a narrow pattern. Of course, once the particles are close together, they tend to aggregate even more by mutual dielectrophoresis (which, by the way, is also due to the above-mentioned secondary field gradients).

It is entirely possible for particles to experience forces with some non-radial components due to mutual dielectrophoresis. This, along with other factors such as the size of the particles and their geometry, and the static charge present on them, can also affect the distribution patterns of the powder on the substrate.

A perfect collimating action would eliminate all horizontal components of the particle motion and give a distribution exactly the same size as the collimator slit. However, the collimator efficiency is directly dependent on the particle size. For this reason, larger particles like magnesium (about 300 microns across) form slightly more uneven and broader distributions compared to smaller particles like iron (about 100 microns in diameter). This holds true even when the center electrode is not energized, unlike the other effects discussed here.

The magnitude of the dipole moment vector, created by the action of the external electric field upon our homogeneous dielectric body, is proportional to the polarizability of the body which in turn is a function of its geometry. Powders in the form of microspheres (eg., glass and iron) all have identical geometries and experience the same acceleration in the drop tower. On the other hand, for a material with randomly shaped constituents, like magnesium, the resulting dielectrophoretic force would fluctuate to some extent among the members of the ensemble of the falling particle samples.

Even though tungsten has irregularly shaped particles, due to its extremely high density the magnitude of the operating acceleration is very low and any variation in this would still not lead to a significant change in trajectory. Drops with aluminum particles with very irregular, elongated geometries were attempted resulting in random distributions.

Since inorganic as well as organic materials can easily pick up a charge in vacuum, through contact potentials or otherwise, an oscillating motion of the particles occurs due to the electrophoretic forces arising under the influence of the high-strength A.C. field. This effect would be especially prominent for light materials like magnesium and PMMA which can develop a high charge-to-mass ratio. This effect can be minimized, though, by increasing the operating frequency of the applied sinusoidal EMF which reduces the magnitude of the oscillations by allowing less time for each cycle.

PMMA microspheres were also utilized in some test runs (see Table 1). However, observations showed the deposition of very little PMMA

on the substrate. Since this polymer tends to collect a static charge very easily, it is possible that this upsets the trajectories of the particles as they are released from the drop device, resulting in only a very small fraction of them entering the collimation slits. This is supported by the observation of a large number of PMMA microspheres trapped in between the collimator plates. The use of anti-static devices did not ameliorate this problem to any significant extent. However, this should not be a problem in space, since the need for a collimator would be eliminated.

It should be noted that in the absence of a fluid medium, there are no viscous or turbulent energy dissipation phenomena and thus no drag force acts on the particles. Since the dielectrophoretic acceleration is independent of the size of the particles, the separation is based on bulk material properties (and on shape to some extent), but not on size.

The residence time of our powders in the separation column was limited to 0.3 seconds, so in order to achieve observable separations our mixtures consisted of materials with large differences in their relevant bulk properties. In the absence of gravity, the residence time would not be a limiting factor and separations based on small differences in these bulk properties should be easily obtainable.

Chapter 5 : Conclusions

It is possible to carry out dielectrophoresis without a specific supporting medium, which in fact offers advantages over conventional electrokinetic techniques due to the absence of fluid disturbances such as convection. Also in such a case, due to the elimination of all drag forces, the particle deflections are governed only by the electrical forces which allow for separations independent of the size based on two bulk properties of the materials, the dielectric constant and the density.

The operating dielectrophoretic force actually gets enhanced due to multiparticle effects. Such observations were also made earlier by Pohl et al.[3], and can now be attributed to significant local field perturbations by the dielectric particles, as indicated by the analysis developed to investigate these discrepancies. Thus, a close proximity of particles to each other leads to observed separations greater than those predicted by the simple theory based on movements of individual particles independently in the field.

Vacuum dielectrophoresis can be utilized as a particulate materials separations technique in a microgravity environment, since residence times in the separation cells would be extremely large compared to those of our investigation and consequently very efficient separations based on differences in density and dielectric constant should be achievable.

Bibliography

1. Pohl, H. A., and Schwar, J. M.,"Factors Affecting Separations of Suspensions in Nonuniform Electric Fields," J. Appl. Phys., **30**, 69 (1959).

2. Pohl, H. A., and Schwar, J. M.," Particle separations by Nonuniform Electric Fields in Liquid Dielectrics," J. Electrochem. Soc., **107**, 383 (1960).

3. Pohl, H. A., and Plymale, C.E.," Continuous Separations of Suspensions by Nonuniform Electric Fields in Liquid Dielectrics," J. Electrochem. Soc., **107**, 390 (1960).

4. Crane, J. S., and Pohl, H. A.," A Study of Living and Dead Yeast Cells Using Dielectrophoresis," J. Electrochem. Soc., **115**, 584 (1968).

5. Debye, P., Debye, P. P., Eckstein, B. H., Barber, W. A., and Arquette, G. J.," Experiments on Polymer Solutions in Inhomogeneous Electric Fields," J. Chem. Phys., **22**,152 (1954).

6. Eisenstadt, M., and Scheinberg, I. H.," Dielectrophoresis of Macromolecules: Determination of the Diffusion Constant of Poly-γ-Benzyl-L-Glutamate," Science, **176**, 1335 (1972).

7. Snyder, R.S., Bier, M., Griffin, R. N., Johnson, A. J., Leidheiser, H., Micale, F. J., Rose, S., Vanderhoff, J. W., and Van Oss, C. J.," Free Fluid Particle Electrophoresis on Apollo 16," Separation and Purification Methods, **2**, 259, (1973).

8. Allen, R. E., Rhodes, P. H., Snyder, R. S., Barlow, G. H., Bier, M., Bigazzi, P. E., Van Oss, C. J., Knox, R. J., Seaman, G. V. F., Micale, F. J., and Vanderhoff, J. W.," Column Electrophoresis on the Apollo-Soyuz Test Project," Separation and Purification Methods, **6**, 1, (1977).

9. Pohl, H. A., " Dielectrophoresis," Cambridge University Press, Cambridge,1978, pp. 6-17, 34-42, and 48-51.

10. Von Hippel, A. R.," Dielectrics and Waves," John Wiley, New York, 1954, pp. 312 and 334.

11. Von Hippel, A. R.," Dielectrics Materials and Applications," John Wiley, New York, 1954, pp. 9-11 and 39.

Table 1

Bulk Properties of Experimental materials

	Specific Gravity	Dielectric constant
Magnesium	1.74	∞
Iron	7.87	∞
Tungsten	19.30	∞
Silica Glass	2.55	5.5
Alumina	3.97	8.6
PMMA (Acrylic)	1.20	2.9

Table 2

Theoretically Predicted Deflections of Experimental Materials

	Calculated using constant accln. (mm.)	Calculated using reiteratively corrected accln. (mm.)
Magnesium	2.83	3.08
Iron	0.63	0.64
Tungsten	0.26	0.26
Silica Glass	1.16	1.20
Alumina	0.89	0.91

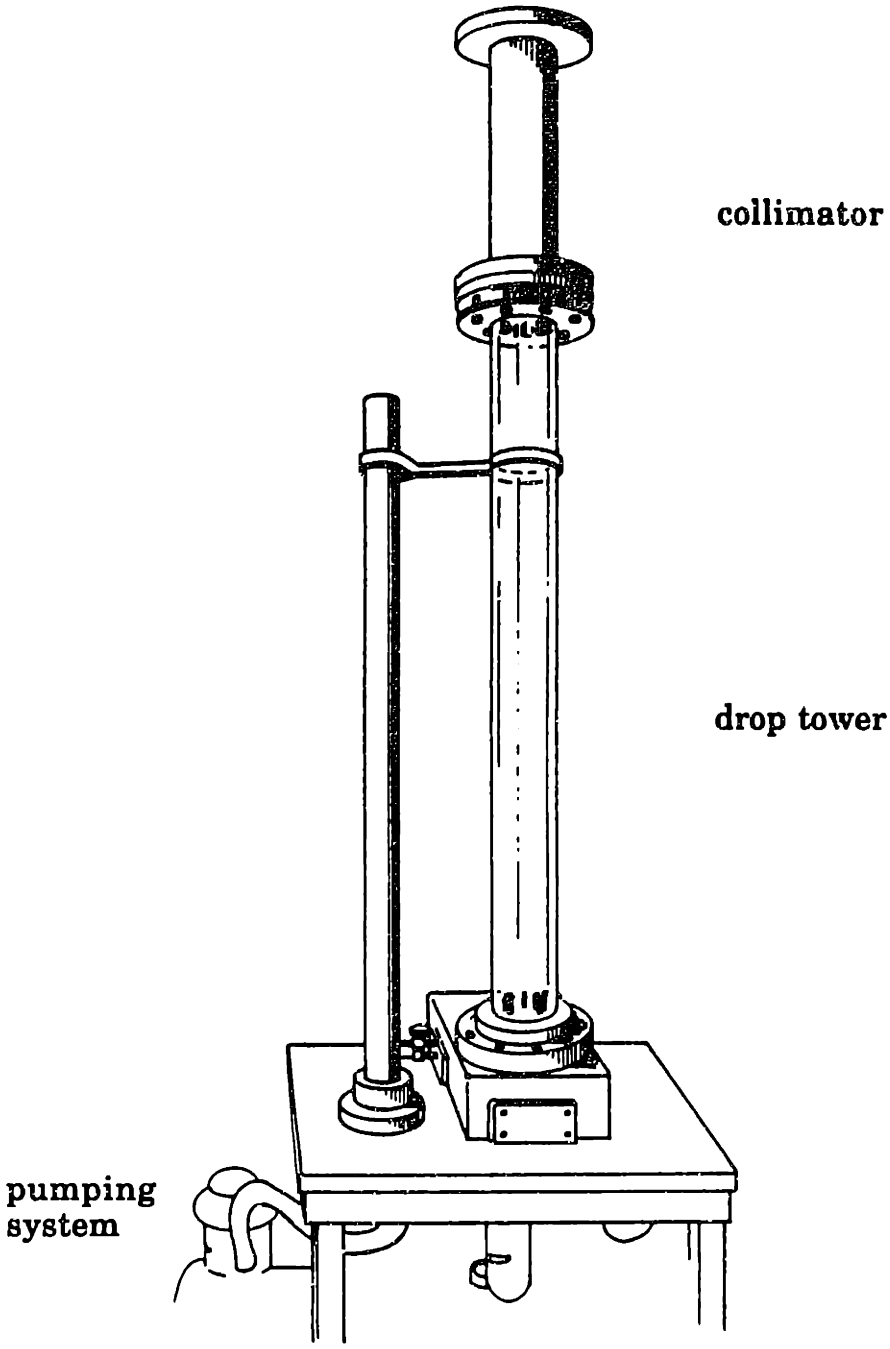

Fig. 1 : Experimental setup
(for explanation, see text)

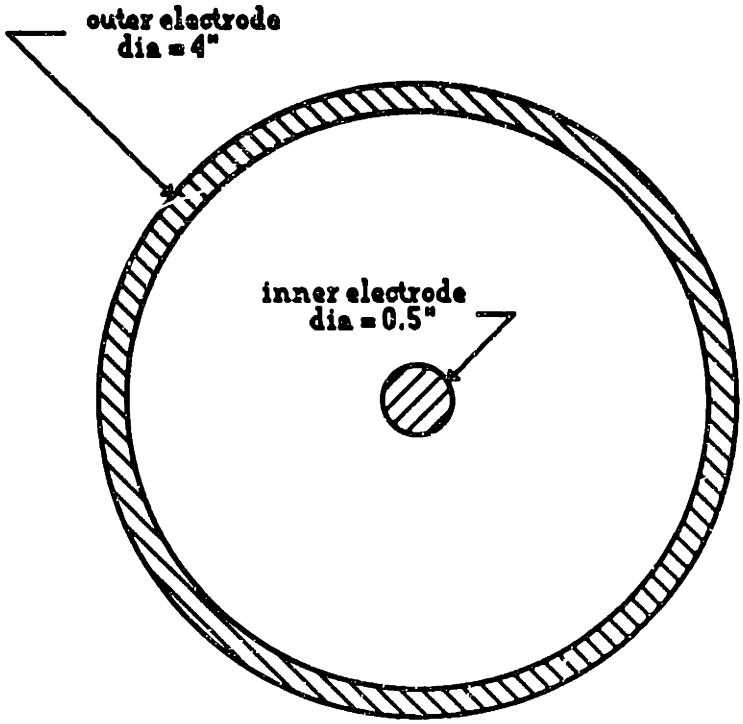

Fig. 2 : Concentric cylindrical electrode configuration : Radial cross-section

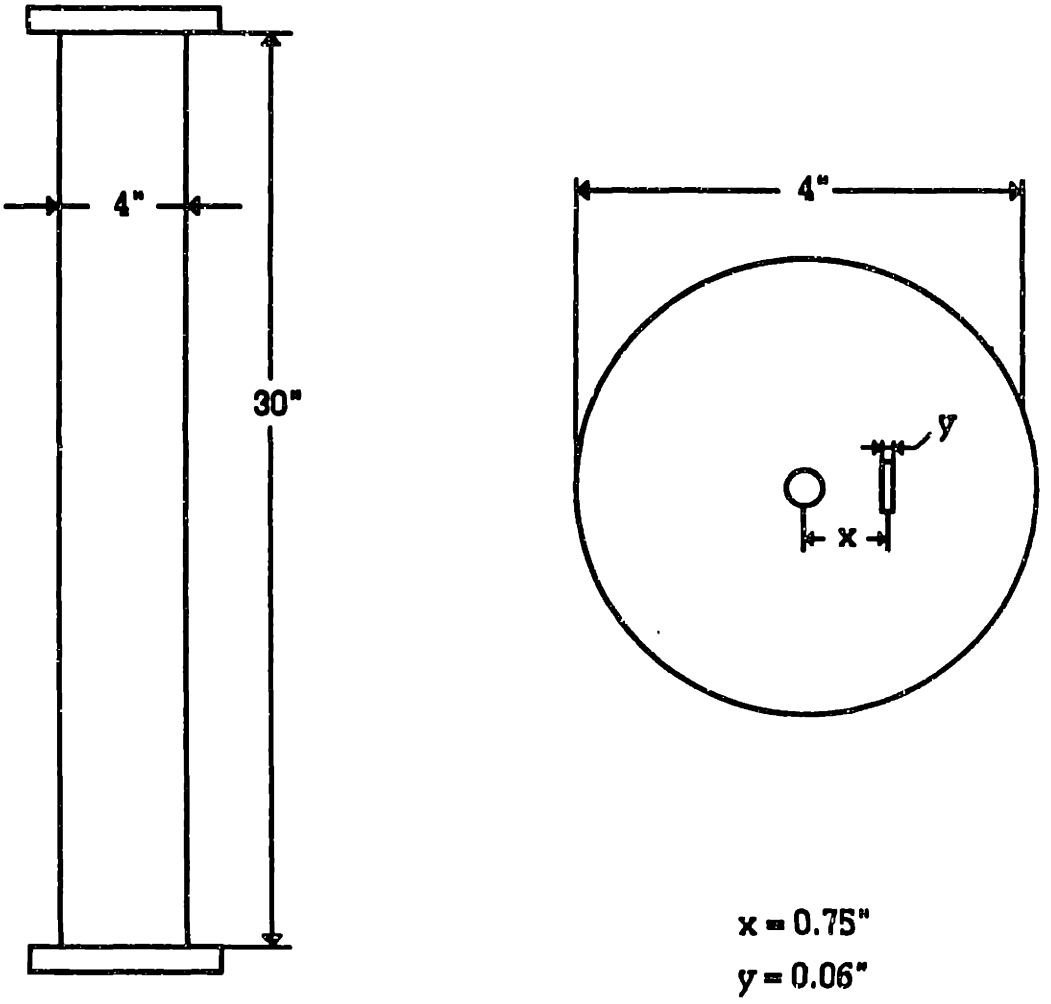

(a) Collimator

(b) Collimation plate

Fig. 3 : Collimation apparatus

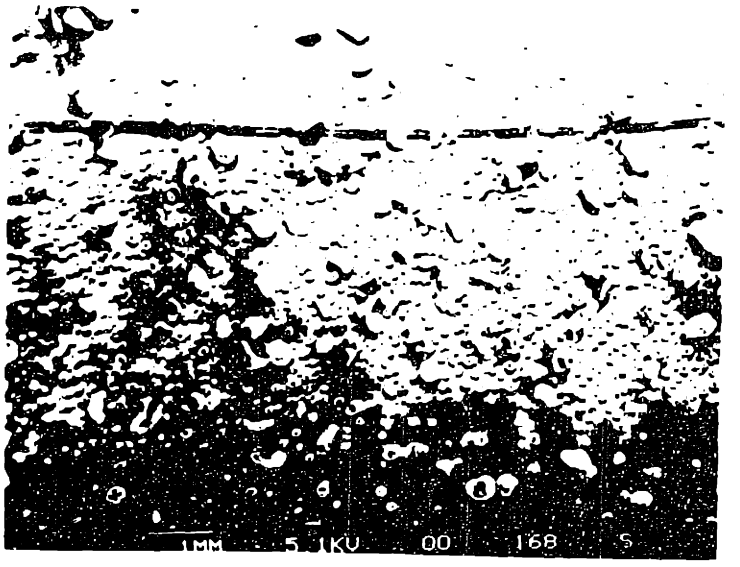

4 (a) : No EMF applied

4 (b) : 10 kV applied

Fig. 4 : Sample SEM photographs of powder distributions on substrate : Magnesium and Alumina

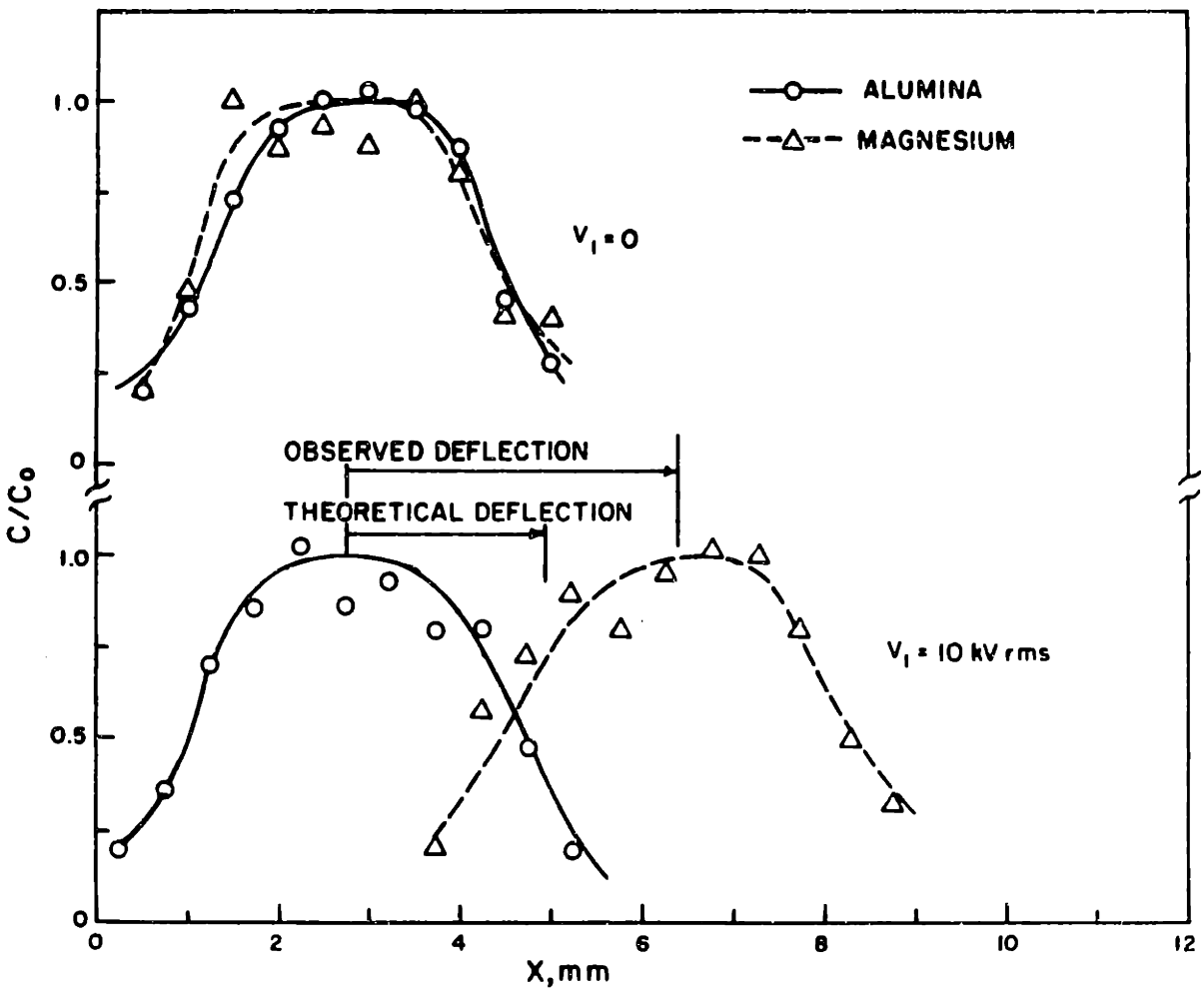

Fig. 5 : Distribution of powders on substrate : Magnesium and Alumina

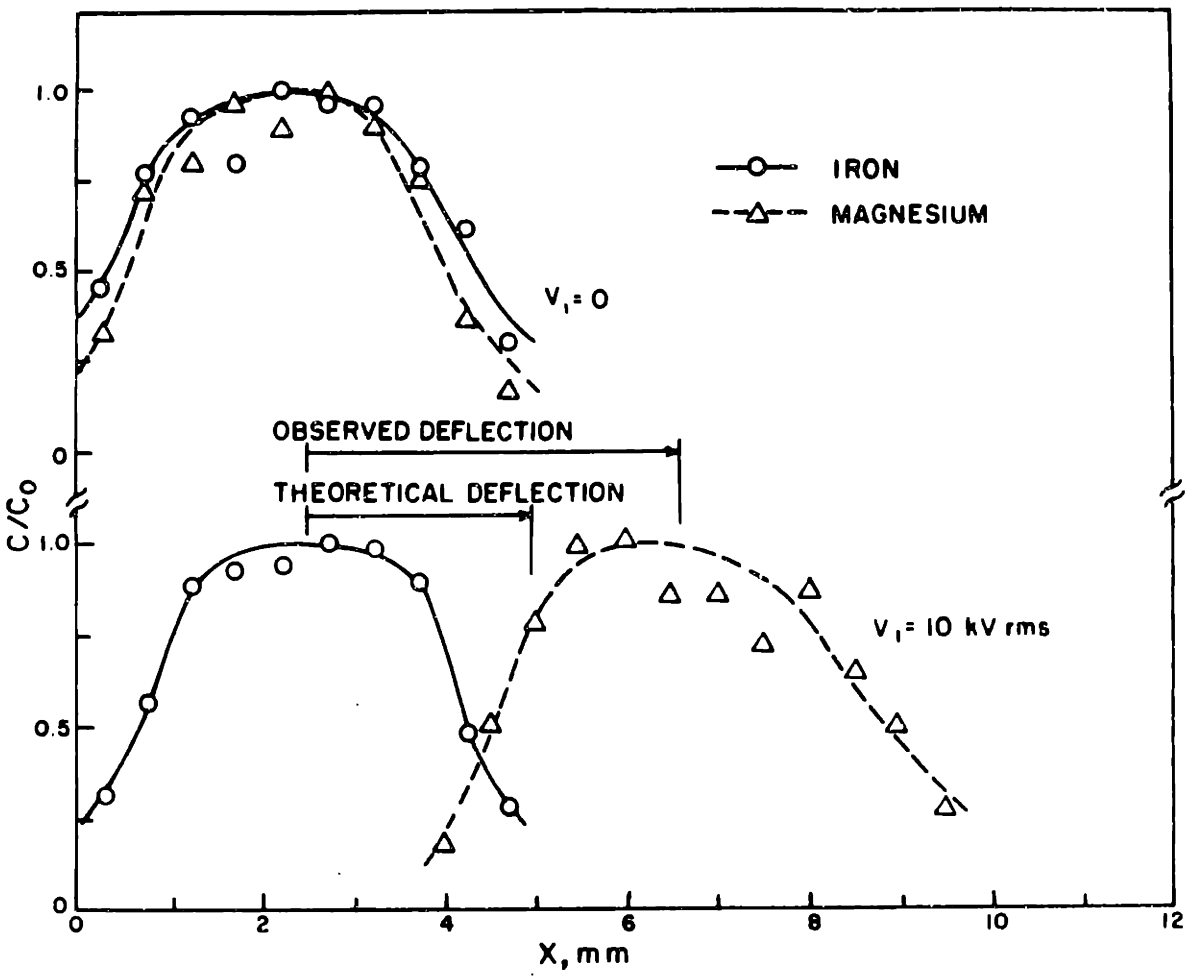

Fig. 6 : Distribution of powders on substrate : Magnesium and Iron

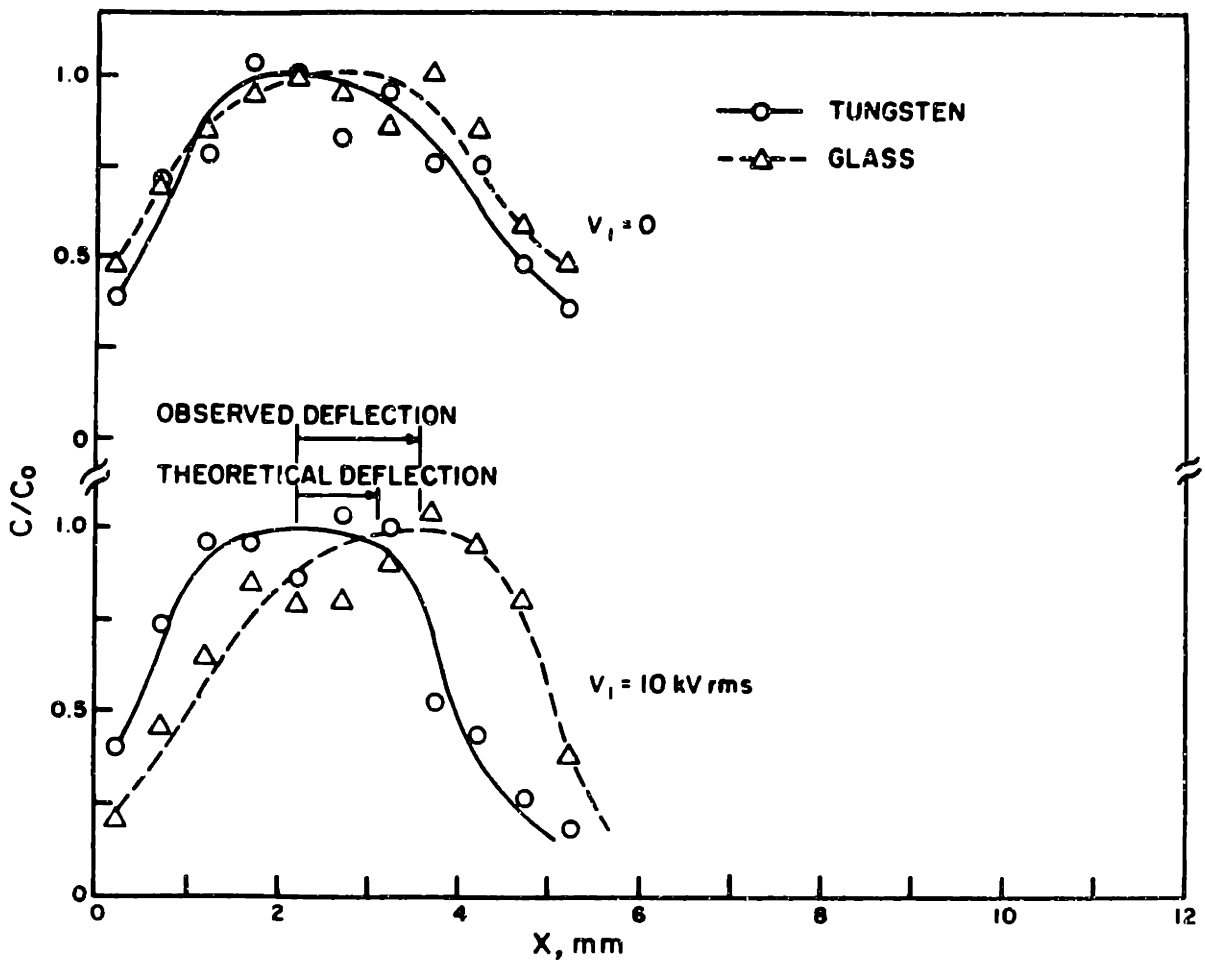

Fig. 7 : Distribution of powders on substrate : Glass and Tungsten

Appendix I

For the theoretical calculations, it was initially assumed that the radial acceleration of the particles is constant for their time of residence in the drop tower. In reality, since the particles move radially inwards under the influence of the dielectrophoretic force, which in turn is a function of the radial position, the acceleration would change continuously with time. To test this assumption, a small computer program was written to calculate the actual distance travelled by a particle by reiteratively applying a correction to the acceleration on the basis of the radial distance travelled by it. The parameters input in the sample program are for magnesium, the material displaying the greatest deflection in the field by virtue of its low density and high dielectric constant, where any discrepancy between the results from the two methods would be the greatest. The results obtained indicated that for the lighter particles (which deflect more in the field), the reiteratively corrected accelerations can result in an increase in deflections by about 5-10% as shown in Table 2.

```
REM       THIS PROGRAM CALCULATES THE ACTUAL DISTANCE
REM       TRAVELLED BY A DIELECTRIC PARTICLE MOVING
REM       RADIALLY INWARDS  UNDER THE INFLUENCE OF  OUR
REM       NONUNIFORM ELECTRIC FIELD BY REITERATIVELY
REM       CALCULATING ITS ACCELERATION AND COMPARES IT TO
REM       THE DISTANCE TRAVELLED BY ASSUMING COSTANT
REM       ACCLN.
REM
REM       MATERIAL COSIDERED : MAGNESIUM
REM
REM       PROGRAM DIELECTROPHORESIS
     OPEN "LPT1:PROMPT" FOR OUTPUT AS #1
     TOTHT = 2.5908
     COLLHT = .762
     G = 9.81
     TIMETOT  = (2*TOTHT/G)^.5
     TIMECOLL = (2*COLLHT/G)^.5
     TIMEFALL = TIMETOT - TIMECOLL
     RAD1 = .00635
     RAD2 = .0508
     RADINIT = .75*.0254
     RHO = 1740
     K1 = 1
     K2 = 1E+10
     EPSL = 8.854E-12
     V1 = 10000
     X = LOG(RAD1/RAD2)
     TEMP1 = 2*(V1^2)/(X^2)
     TEMP2 = 3*EPSL*K1*(K2-K1)/((K2+(2*K1))*2*RHO)
     RAD = RADINIT
     DELR = 0
     T =0
     VELI = 0
10:
     ACCN = TEMP1*TEMP2/(RAD^3)
     IF(T>0) GOTO 30
     DELRAD1 = (.5*ACCN*(TIMEFALL)^2)*1000

20:
     PRINT #1,"DEFLECTION OF A MAGNESIUM PARTICLE "
     PRINT #1,"INITIAL RADIUS = .075 INCHES"
     PRINT #1,"CALCULATED BY APPLYING CONSTANT
                    ACCLN  = ";DELRAD1;"mm"
30:
     DELTIME = .001
     VELF = VELI + ACCN*DELTIME
     DELR = ((VELF^2)-(VELI^2))/(2*ACCN)
     RAD = RAD-DELR
     VELI = VELF
      T = T+DELTIME
```

```
    IF(T >= TIMEFALL) GOTO 40
    GOTO 10
40:
    DELRAD2 = (RADINIT-RAD)*1000

50:
    PRINT#1, "CALCULATED BY REITERATIVELY CORRECTING
    ACCELERATION = "
    PRINT#1,  DELRAD2;"mm"
60:
    CLOSE#1
    END
```

Appendix II

The field at radius r, in a system with concentric cylindrical electrodes, with the inner electrode of radius r_1 at potential V_1 and the outer electrode r_2 at ground state, is

$$\mathbf{E}_r = \frac{-V_1}{r \ln(r_1/r_2)} \mathbf{r}_0$$

The gradient of the square of the field's magnitude can be obtained by simply evaluating its variation in the radial direction (since this field varies only in that direction).

Consider the field at a point at radius $r-\delta$ from the axis of the electrodes :

$$\mathbf{E}_{r-\delta} = \frac{-V_1}{(r-\delta) \ln(r_1/r_2)} \mathbf{r}_0$$

$$\text{We have } \nabla|\mathbf{E}_r|^2 = \lim(\delta->0) \frac{|\mathbf{E}_r|^2 - |\mathbf{E}_{r-\delta}|^2}{\delta}$$

$$= \lim(\delta->0) \frac{1}{\delta} \left\{ \frac{V_1^2}{r^2 \left[\ln(r_1/r_2)\right]^2} - \frac{V_1^2}{(r-\delta)^2 \left[\ln(r_1/r_2)\right]^2} \right\} \mathbf{r}_0$$

$$= \lim(\delta->0) \frac{1}{\delta} \frac{V_1^2}{\left[\ln(r_1/r_2)\right]^2} \left\{ \frac{1}{r^2} - \frac{1}{(r-\delta)^2} \right\} \mathbf{r}_0$$

$$= \lim(\delta->0) \frac{1}{\delta} \frac{V_1^2}{\left[\ln(r_1/r_2)\right]^2} \left\{ \frac{r^2+\delta^2-2r\delta-r^2}{r^2(r-\delta)^2} \right\} \mathbf{r}_0$$

$$= \lim(\delta \to 0)\ \frac{1}{\delta}\frac{V_1^2}{\left[\ln(r_1/r_2)\right]^2}\left\{\frac{(\delta^2/r) - 2\delta}{r(r-\delta)^2}\right\} r_0$$

$$= \frac{V_1^2}{\left[\ln(r_1/r_2)\right]^2}\left\{\frac{-2}{r^3}\right\} r_0$$

$$\text{Thus } \nabla|E_r|^2 = \frac{-2V_1^2}{r^3\left[\ln(r_1/r_2)\right]^2} r_0$$

This treatment assumed the absence of any other local distortions of the external electric field, which in reality may exist due to the dipole fields set up by other dielectric bodies in the system. In our case, the only perturbations which are of any interest are those which affect radial components of the acceleration experienced by the reference particle (i.e. by causing variations in the radial field gradients). It should be noted at this point that even though the external field has no other components other than the radial one, it may be possible to obtain field gradients in other directions entirely due to the presence of other dielectric bodies.

The strength of a dipole field at a distance l from the center of a dipole induced by an electric field **E** in a dielectric body of dielectric permittivity ε_2 paced in a medium of dielectric permittivity ε_1 can be shown to have the components (denoted by the superscripts R and θ)[10]

$$\left|E^{d,R}\right| = \frac{\mu . l_o}{2\Pi\varepsilon_1 l^3}$$

$$\left|\mathbf{E}^{d,\theta}\right| = \frac{|\mu|\cos\theta}{4\Pi\varepsilon_1 l^3}$$

where $\mathbf{l}_0$ is a unit vector along the line connecting this center to our point of interest. θ obviously is the angle between $\mathbf{l}_0$ and μ. If we assume the body to be a uniformly and homogeneously polarizable sphere, consistent with the basic assumptions of our theoretical analysis (Chapter 2), then its center is coincident with that of the dipole.

μ is the dipole moment vector whose magnitude in turn is also a function of the external electric field

$$\mu = (\alpha v)\mathbf{E}$$

where α is the polarizability and v the volume of the body. For a small sphere of radius c (Chapter 2)

$$\alpha = 3\varepsilon_1 \left(\frac{\varepsilon_2 - \varepsilon_1}{\varepsilon_2 + 2\varepsilon_1}\right)$$

Both the R and θ components of the dipole field would actually produce local distortions in the radial components of the external electric field, if these components are acting in the radial direction of our system. To demonstrate the effects of the dipole field, however, only the R component will be considered, since, being stronger, it would contribute to the perturbations to a more significant extent. This component from any particle will obviously have the strongest effect on the external field at any point P if it acts in the same direction as the field itself acting through that point, i.e. the center of the dipole and P are collinear in the radial direction of the system under consideration. If the point P is at radius p, the center of the dipole at a distance l from P can then occupy two radial positions, $p + l$ and $p - l$.

Case 1: Center of dipole at p - l

The total electric field at point P (E_p^T) is due to the dipole field and the external field

$$E_p^T = (E_p)^{ext} + (E_p)^{d,R}$$

$$= \frac{-V_1}{p \ln(r_1/r_2)} r_o + \frac{\mu . l_o}{2\Pi\varepsilon_1 l^3} r_o$$

$$= \frac{-V_1}{p \ln(r_1/r_2)} r_o + 4\Pi c^3 \varepsilon_1 \left(\frac{\varepsilon_2 - \varepsilon_1}{\varepsilon_2 + 2\varepsilon_1}\right) \frac{1}{2\Pi\varepsilon_1 l^3} \frac{-V_1}{(p-l)\ln(r_1/r_2)} r_o$$

$$= \frac{-V_1}{p \ln(r_1/r_2)} \left\{ 1 + 2(c/l)^3 \left(\frac{\varepsilon_2 - \varepsilon_1}{\varepsilon_2 + 2\varepsilon_1}\right) \frac{1}{1-(l/p)} \right\} r_o$$

Since c << p and $[(\varepsilon_2 - \varepsilon_1)/(\varepsilon_2 + 2\varepsilon_1)] < 1$, the second term inside the brackets is significant compared to the first one if and only if l is not much larger than c (it, of course cannot be smaller than c) , which in turn implies that l must be much smaller than p or (l / p) << 1 whereby

$$\Rightarrow \quad E_p^T = \frac{-V_1}{p \ln(r_1/r_2)} \left\{ 1 + 2(c/l)^3 \left(\frac{\varepsilon_2 - \varepsilon_1}{\varepsilon_2 + 2\varepsilon_1}\right) \right\} r_o$$

Case 2: Center of dipole at p + l

By indulging in reasoning similar to that of case 1, we can arrive at exactly the same result. Thus, for the scenario (of the dipole being on the same radial vector as P) considered, a dielectric body can significantly

perturb the local field only at points very close to itself and the relative radial placement of the body, for a given distance from the reference point, does not significantly alter the magnitude of the perturbation.

To get some quantitative evaluation of the magnitude in the variation of the field gradients by considering these "multiparticle effects", let us choose a simple case of 3 particle (each of radius c) all lying on the same radial vector. Let the center of the reference particle (for which we want to evaluate the effect of the local field inhomogeneities) be at radius r, and the centers of the other two particles at radial positions of r - x (particle 1)and r + x (particle 2). Now let us calculate the total electric field ($\mathbf{E}^T$) at the positions r - c and r + c (i.e. the radial positions of the extreme ends of the reference body).

Since the dipole field strength varies as the inverse of third power of the distance from the dipole, we need to consider only the contribution from particle 1 at r - c and particle 2 at r + c. This is actually a conservative approach since in reality particle will have a small effect effect at r + c and particle 2 at r - c, which would enhance the field perturbations.

So, at radial position r - c

$$\mathbf{E}^T_{r-c} = \frac{-V_1}{(r-c)\,\ln(r_1/r_2)} \left\{ 1 + 2\left(\frac{c}{x-c}\right)^3 \left(\frac{\varepsilon_2-\varepsilon_1}{\varepsilon_2+2\varepsilon_1}\right) \right\} \mathbf{r}_o$$

Similarly at r + c

$$\mathbf{E}^T_{r+c} = \frac{-V_1}{(r+c)\,\ln(r_1/r_2)} \left\{ 1 + 2\left(\frac{c}{x-c}\right)^3 \left(\frac{\varepsilon_2-\varepsilon_1}{\varepsilon_2+2\varepsilon_1}\right) \right\} \mathbf{r}_o$$

$$\nabla|\mathbf{E}_r|^2 = \lim(c\to 0)\ \frac{|\mathbf{E}_{r+c}|^2 - |\mathbf{E}_{r-c}|^2}{2c}\,\mathbf{r}_o$$

$$= \lim(c\to 0)\ \frac{V_1^2}{\left[\ln(r_1/r_2)\right]^2}\left(1+2\left(\frac{c}{x-c}\right)^3\left(\frac{\varepsilon_2-\varepsilon_1}{\varepsilon_2+2\varepsilon_1}\right)\right) \times \frac{1}{2c}\left\{\frac{1}{(r+c)^2} - \frac{1}{(r-c)^2}\right\}\mathbf{r}_o$$

$$\text{Now } \lim(c\to 0)\ \frac{1}{2c}\left\{\frac{1}{(r+c)^2} - \frac{1}{(r-c)^2}\right\}$$

$$= \lim(c\to 0)\ \frac{1}{2c}\left\{\frac{-4cr}{\left[r^2-c^2\right]^2}\right\} = \frac{-2}{r^3}$$

$$\Rightarrow\ \nabla|\mathbf{E}_r|^2 = \frac{-2V_1^2}{r^3\left[\ln(r_1/r_2)\right]^2}\left\{1+2\left(\frac{c}{x-c}\right)^3\left(\frac{\varepsilon_2-\varepsilon_1}{\varepsilon_2+2\varepsilon_1}\right)\right\}\mathbf{r}_0$$

If $\varepsilon_2 >> \varepsilon_1$ and letting $x = 3c$ (a rough estimate of the radius to radius distance between some of the particles in our particle distribution photographs) we get an enhancement of 56% in the resulting dielectrophoretic force. On the other hand, for $x = 4c$, the additional effect results in an increment of only 7%. Thus, we see that the effect of the secondary electric field is a very strong function of the distance from the relevant particle.